Contrib Mineral Petrol (1988) 98:374–389

Contributions to Mineralogy and Petrology

The geochemistry and petrogenesis of K-rich alkaline volcanics from the Batu Tara volcano, eastern Sunda arc

A.J. Stolz[1], R. Varne[1], G.E. Wheller[1], J.D. Foden[2], and M.J. Abbott[3]

[1] Department of Geology, University of Tasmania, Box 252C, G.P.O. Hobart, Tasmania 7001, Australia
[2] Department of Geology, University of Adelaide, Box 498, G.P.O. Adelaide, S.A. 5001, Australia
[3] School of Earth Sciences, Flinders University, Bedford Park, S.A. 5042, Australia

Abstract. Mineralogical, major and trace element, and isotopic data are presented for leucite basanite and leucite tephrite eruptives and dykes from the Batu Tara volcano, eastern Sunda arc. In general, the eruptives are markedly porphyritic with phenocrysts of clinopyroxene, olivine, leucite ± plagioclase ± biotite set in similar groundmass assemblages. These K-rich alkaline volcanics have high concentrations of large-ion-lithophile (LIL), light rare earth (LRE) and most incompatible trace elements, and are characterized by high $^{87}Sr/^{86}Sr$ (0.70571–0.70706) and low $^{143}Nd/^{144}Nd$ (0.512609–0.512450) compared with less alkaline volcanics from the Sunda arc. They also display the relative depletion of Ti and Nb in chondrite-normalized plots which is a feature of subalkaline volcanics from the eastern Sunda arc and arc volcanics in general. Chemical and mineralogical data for the Batu Tara K-rich rocks indicate that they were formed by the accumulation of variable amounts of phenocrysts in several melts with different major and trace element compositions. The compositions of one of these melts estimated from glass inclusions in phenocrysts is relatively Fe-rich ($100\ Mg/(Mg+Fe^{2+})=48$–51) and is inferred to have been derived from a more primitive magma by low-pressure crystal fractionation involving olivine, clinopyroxene and spinel. Mg-rich ($mg \sim 90$) and Cr-rich (up to 1.7 wt. % Cr_2O_3) zones in complex oscillatory-zoned clinopyroxene phenocrysts probably also crystallized from such a magma. The marked oscillatory zoning in the clinopyroxene phenocrysts is considered to be the result of limited mixing of relatively 'evolved' with more primitive magmas, together with their phenocrysts, along interfaces between discrete convecting magma bodies.

Introduction

K-rich alkaline rocks are a rare but petrologically important manifestation of volcanism both in active island arcs and intraplate environments.

Ultrapotassic or K-rich alkaline rocks have recently been divided into three principal groups on the basis of major and trace element compositions (Foley et al. 1987). Group I rocks (e.g. Western Australia: Jaques et al. 1984; Nixon et al. 1984; Antarctica: Sheraton and Cundari 1980; southeast Spain: Venturelli et al. 1984) are characterized by low CaO and Al_2O_3 and extreme enrichment in compatible elements. Group II rocks (e.g. New South Wales: Cundari 1973; West Eifel: Mertes and Schmincke 1985; western Uganda: Mitchell and Bell 1976) are distinguished from Group I rocks by their higher CaO and from Group III rocks by the higher Al_2O_3 of the latter. In addition, Group III rocks, which include eruptives from Italy (Cox et al. 1976; Hawkesworth and Vollmer 1979; Holm et al. 1982; Poli et al. 1984; Rogers et al. 1985) and Indonesia (Foden and Varne 1980; Nicholls and Whitford 1983; Varne and Foden 1986) generally display quite marked relative depletions of Nb, Ta and Ti and less enrichment of LRE and incompatible elements in chondrite-normalized plots compared with Group II K-rich alkaline eruptives. This relative depletion of high field strength elements (HFSE) is also a distinctive feature of arc volcanics in general (Pearce and Cann 1973; Perfit et al. 1980). Group III K-rich alkaline rocks from the Sunda arc appear, therefore, to bear the geochemical imprint of the tectonic regime in which they were generated (Foden and Varne 1980), unlike the Italian volcanics which have no clear spatial relationship to an active subduction zone (Cundari 1980).

Even where the spatial relationship between K-rich volcanism and a Benioff zone is clearly defined, as in the Sunda arc, there is considerable debate about the role of subduction in the genesis of the K-rich rocks. Whitford et al. (1979) proposed that K-rich leucite-bearing eruptives of Muriah and Ringgit Beser in Java were generated in response to subduction of Indian Ocean crust beneath the Asian plate, and that the occurrence of these K-rich volcanics on the northern side of the Sunda arc was consistent with their occurrence where the subducting plate is deeper than it is beneath medium- or high-K calcalkaline volcanics. In contrast, Foden and Varne (1980) showed that no simple relationship exists between K_2O content and depth to Benioff zone in the eastern Sunda arc.

Here we document the mineralogy and geochemistry of leucite basanites and leucite tephrites from Batu Tara volcano, a small volcanic island located about 50 km north of the island of Lembata (formerly called Lomblen) in the eastern Sunda arc (Fig. 1). The volcano is located approximately 230 km above the inferred Benioff zone in a region where the arc crust is relatively young and thin (Ben Avraham and Emery 1973; Curray et al. 1977).

The uninhabited island of Batu Tara is the steep-sided summit of an active stratovolcano and has a small summit crater which is open to the east (Brouwer 1940). Although

Offprint requests: A.J. Stolz

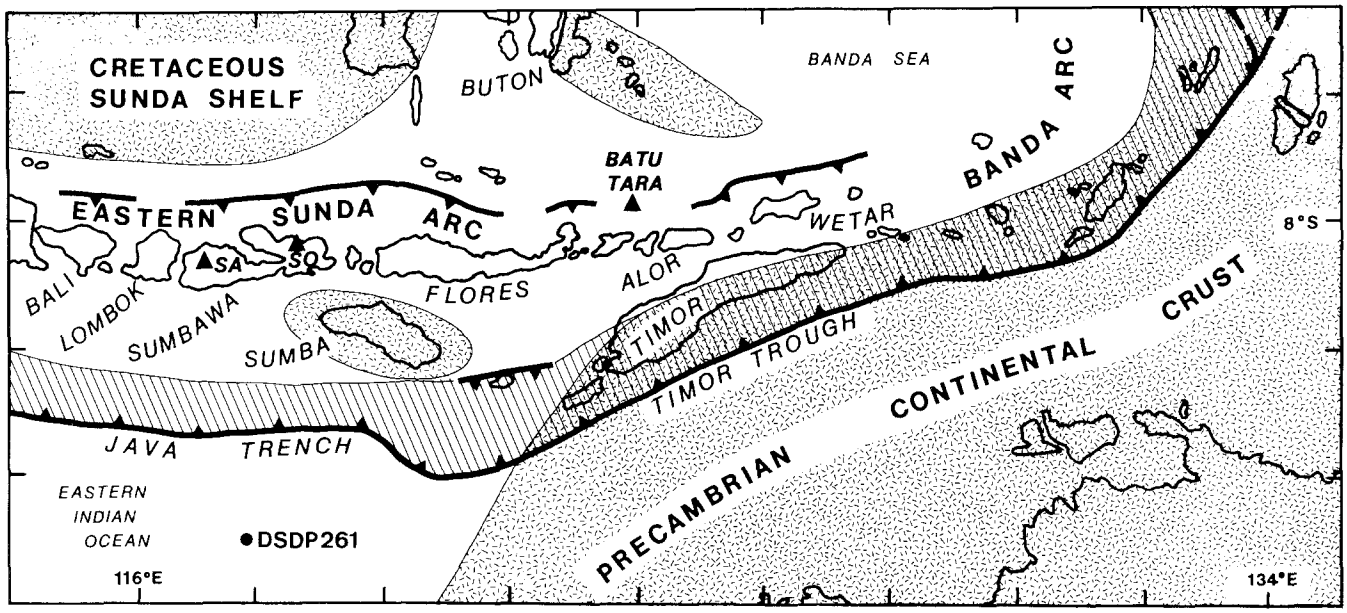

Fig. 1. Map of the eastern Sunda arc (from Varne and Foden 1986) showing the location of the K-rich alkaline volcanoes (solid triangles) Batu Tara, Soromundi (SO) and Sangenges (SA)

only its topmost 750 meters is exposed, the base of the island lies about 3,000 meters below sea level. The island is built of lava flows, intercalated with ash and breccia deposits, and cut by many dykes. The most recently reported eruption of lavas and bombs was in 1847–1852. Most of our samples were collected along the eastern flanks of the island in March 1984, but it is uncertain if any of the material collected was from the historical eruptions. Additional material, collected by H.A. Brouwer in 1937, was obtained from the University of Amsterdam collection.

Petrography

The exposed Batu Tara eruptives can be divided into three groups on petrographic, chemical and temporal (Brouwer 1940) grounds. The oldest eruptives exposed above sea-level are a series of leucite basanite lavas (Group 1) which have been intruded by dykes of leucite basanite and leucite tephrite (Group 2). Brouwer's (1940) youngest eruptive group is composed of biotite leucite tephrites (Group 3). Leucite basanites are distinguished from leucite tephrites by the absence of olivine in the latter (Sorensen 1974).

The oldest (Group 1) leucite basanites are vesicular and strongly porphyritic (30–60 percent phenocrysts) with euhedral olivine, clinopyroxene and leucite phenocrysts set in a groundmass composed of plagioclase, leucite, clinopyroxene, olivine, titanomagnetite, and minor amphibole, biotite and apatite. Clinopyroxene phenocrysts commonly display intricate concentric and hourglass zoning (Fig. 2a), and contain inclusions of olivine, Ti-poor magnetite, apatite, leucite and glass. Cr-rich spinel occasionally occurs as inclusions in olivine phenocrysts in one rock (67148). To our knowledge Cr-spinel has not been recognized previously in other suites of arc-related leucite-bearing volcanic rocks. Encrusting aggregates of leucite microphenocrysts around several phenocrysts of clinopyroxene and olivine (Fig. 2b) suggest a leucite-producing reaction relationship between the early crystallized ferromagnesian phases and residual melt.

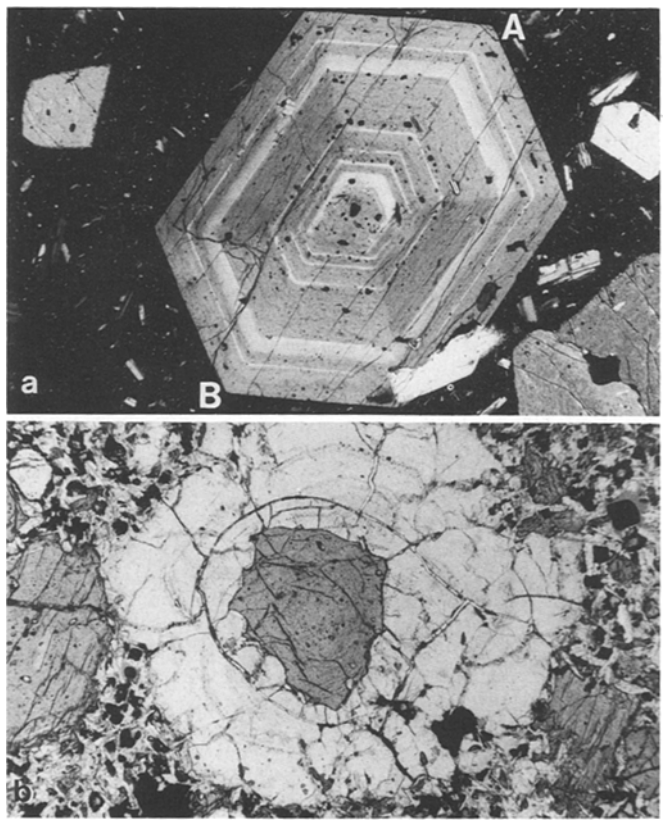

Fig. 2. a Photomicrograph of a clinopyroxene phenocryst from leucite basanite 67148 showing oscillatory and sector zoning. Intracrystalline compositional variations depicted in Fig. 4 are for a traverse from A to B. Distance from A to B is 3 mm. Crossed-polarized light; **b** Photomicrograph showing a reaction rim of leucite around olivine. Field width 4 mm. Plane-polarized light

The Group 2 dyke rocks differ most markedly from the Group 1 eruptives in their greater modal plagioclase and in their possession of plagioclase as a phenocryst phase. Leucite basanite dykes grade into leucite tephrite dykes with

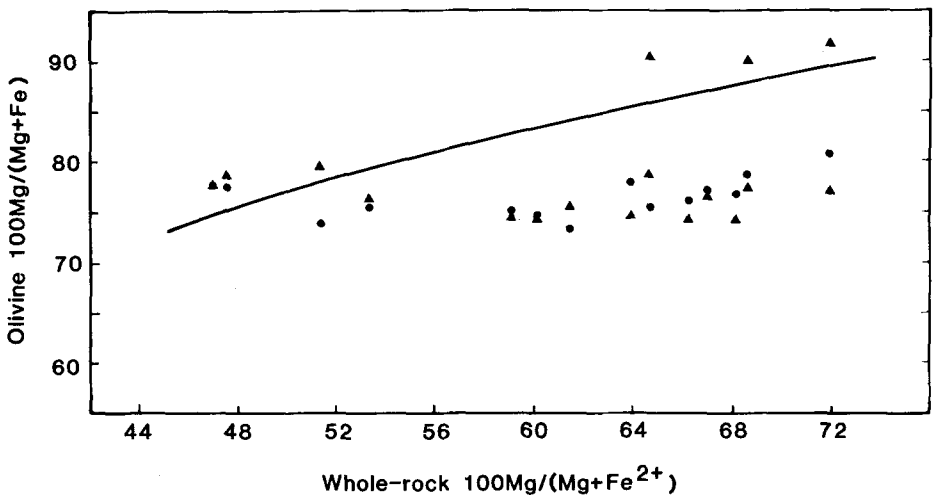

Fig. 3. Variation of maximum measured 100 Mg/(Mg+Fe) of coexisting olivine (*dots*) and clinopyroxene (*triangles*) phenocrysts with 100 Mg/(Mg+Fe^{2+}) of the host rock. The curve represents the variation of liquidus olivine *mg*-value with changing melt 100 Mg/(Mg+Fe^{2+}) assuming $K_{D\,Fe-Mg}^{Ol-liq}=0.30$ (Roeder and Emslie 1970)

decreasing modal olivine. The groundmass mineralogy of the dykes is similar to that in the older flows but more coarse-grained.

The Group 3 biotite leucite tephrites are characterized by phenocrysts of biotite, clinopyroxene, plagioclase, leucite, magnetite and rare olivine in a groundmass of plagioclase, leucite, clinopyroxene, magnetite ± glass.

Mineralogy

Representative analyses of phenocryst and groundmass phases from members of the three petrographic groups are given in Table 1. Analyses represent averages of two to three point analyses performed on a JEOL JXA50A electron microprobe in the Central Science Laboratory, University of Tasmania. Reduction of the EDS spectra involved peak integration and ZAF corrections. Further details of the microprobe analytical techniques and detection limits are provided by Ware (1981).

Olivine phenocrysts from all rock types range in composition from *mg* = 81 to 74 (*mg* = 100 Mg/(Mg+∑Fe) where ∑Fe = total Fe as Fe^{2+}). Olivines are generally unzoned and fall within a very restricted compositional range (2–3 mole % Fo) in individual rocks. Coexisting clinopyroxene phenocrysts have similar *mg* values and are commonly unzoned. However, cores and oscillatory zones of some clinopyroxene phenocrysts are considerably more magnesian (*mg* = 88–92), Cr-rich (up to 1.7 wt. % Cr_2O_3), and depleted in Ti and Al compared with adjacent growth zones and associated unzoned phenocrysts (e.g. Table 1, B4155). All clinopyroxene phenocrysts (including the Cr-rich cores) are characterized by low Al^{vi}/Al^{iv} and Na contents indicating minimal Ca-Tschermak and jadeite substitution. This could reflect relatively low pressures of crystallization. However, crystallographic studies of clinopyroxene phenocrysts from a variety of volcanics suggest that the K/Na and Fe^{2+}/Fe^{3+} of the melt may also exert a significant effect on clinopyroxene compositions (Dal Negro et al. 1985, 1986).

The oscillatory zoning in the clinopyroxene phenocrysts (Figs. 2a and 4) generally is characterized by sharp chemically discontinuous boundaries between adjacent zones. The relatively low-*mg* zones may display trends either to slightly more Fe-rich or Mg-rich compositions from core to rim, but marked Fe enrichment only occurs near the crystal margins.

An important observation from the mineralogical data is that the most magnesian cores of olivine and clinopyroxene phenocrysts, from rocks that span a considerable range of *M* (100 Mg/(Mg+Fe^{2+})) values (*M* = 48–72), define a very restricted range of compositions (Fig. 3). The compositions of clinopyroxene and olivine phenocrysts from rocks at the extremes of this whole-rock compositional range (67132 and 67146, Tables 1 and 2) are virtually identical.

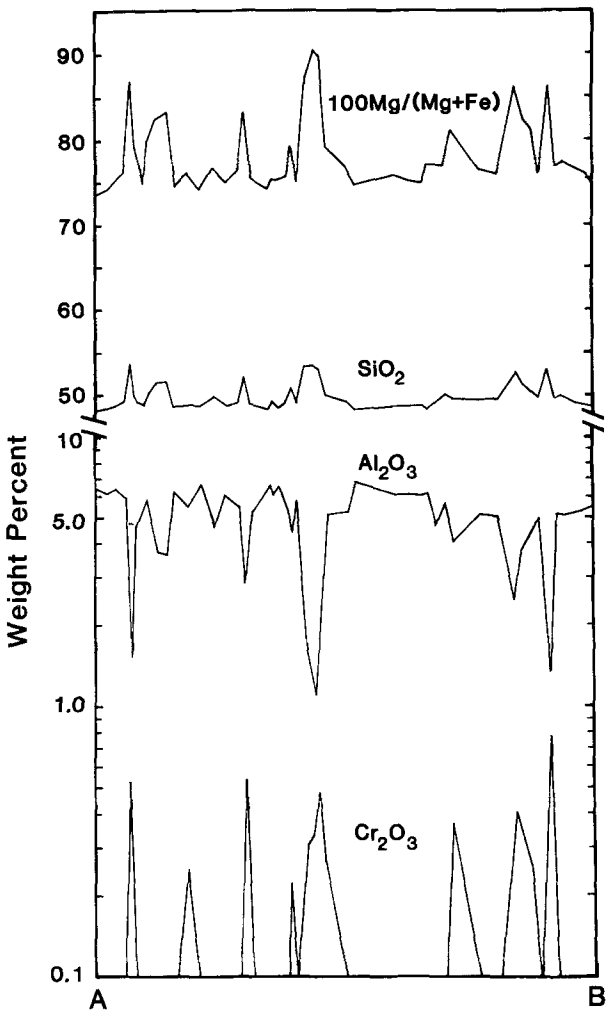

Fig. 4. Variation of 100 Mg/(Mg+Fe), SiO_2, Al_2O_3 and Cr_2O_3 along a traverse line (A–B) across a clinopyroxene phenocryst in leucite basanite 67148 (see *Fig. 2a*)

The compositions of phenocryst and groundmass leucites from all rock types are very similar and characterized by only minor Na, Ca and Fe substitution. The total Fe contents of the leucites (generally less than 0.5 wt. % Fe_2O_3) are significantly lower than those in K-rich rocks from Leucite Hills, Wyoming (Kuehner et al. 1981), but similar to those in lamproites from Gaussberg (Foley

Table 1. Representative analyses of phenocryst and some groundmass phases

	Group 1												Group 2				Group 3					
	B4155			67132							67148		67146				B4200					
	Ol PC	Cpx PC	Cpx PR	Ol PC	Cpx PC	Lc PC	Timt PC	Timt G	Amp G	Mica G	Ol PC	Sp Inc	Ol PC	Cpx PC	Plag PC	Lc PC	Ol PC	Cpx PC	Plag PC	Mica PC	Mt PC	San G
SiO_2	39.16	54.01	49.22	38.87	49.05	55.50			41.55	39.96	38.66		38.34	49.38	45.14	55.30	38.29	51.52	47.18	36.45		63.69
TiO_2			1.02		0.79		6.39	17.45	2.18	2.85		0.61		1.00				0.23		4.72	4.99	0.16
Al_2O_3		1.51	5.34		5.32	22.98	16.82	2.97	10.34	13.59		10.13		5.30	34.44	22.82		3.14	33.41	15.94	5.83	20.49
Cr_2O_3		0.96	0.18				2.02					38.80										
Fe_2O_3*							37.69	31.80				20.09									54.32	
FeO	17.93	2.74	7.56	21.15	7.25	0.52	31.74	46.91	12.74	11.95	22.10	23.63	20.80	6.66	0.75	0.40	23.78	7.39	0.58	12.96	30.99	0.35
MnO	0.32			0.34				0.87	0.26		0.29		0.30				0.78	0.22			0.46	
MgO	42.31	16.97	13.78	40.22	13.81		5.35		14.04	15.26	39.45	6.73	40.11	13.81			37.64	14.59		16.40	3.41	
CaO	0.30	23.95	22.70	0.25	22.87	0.24			11.72		0.17		0.46	22.84	18.31	0.29	0.12	22.91	16.98			1.74
Na_2O			0.20		0.24				2.67	1.19					1.17	0.28			1.79	0.37		3.23
K_2O						21.01			1.67	9.19					0.19	20.79			0.21	9.27		9.78
Total	100.02	100.14	100.00	100.83	99.33	100.25	100.01	100.00	97.17	93.99	100.67	99.99	100.01	98.99	100.00	99.88	100.61	100.00	100.15	96.11	100.00	99.42
Oxygens	4	6	6	4	6	6	32	32	23	22	4	32	4	6	32	6	4	6	32	22	32	32
Si	0.998	1.963	1.834	0.997	1.839	2.009			6.260	5.940	0.997		0.992	1.836	8.367	2.009	0.999	1.913	8.678	5.356		11.623
Ti			0.029		0.022		1.294	3.912	0.247	0.319		0.125		0.028				0.006		0.521	1.086	0.021
Al		0.065	0.234		0.235	0.981	5.341	1.042	1.836	2.380		3.258		0.232	7.521	0.977		0.137	7.242	2.760	1.990	4.406
Cr		0.028	0.005									8.366										
Fe^{3+}							7.641	7.133				4.124									11.836	
Fe^{2+}	0.382	0.083	0.236	0.454	0.227	0.016	7.149	11.694	1.605	1.486	0.477	5.391	0.450	0.207	0.116	0.012	0.519	0.230	0.090	1.593	7.504	0.054
Mn	0.007			0.007				0.220	0.033		0.006		0.007				0.017	0.007			0.114	
Mg	1.607	0.920	0.765	1.538	0.771		2.146		3.153	3.381	1.517	2.738	1.547	0.765			1.463	0.808		3.592	1.471	
Ca	0.008	0.933	0.906	0.007	0.919	0.009			1.892		0.005		0.013	0.950	3.635	0.011	0.003	0.912	3.346			0.340
Na					0.018				0.779	0.343					0.422	0.020			0.638	0.104		1.142
K						0.971			0.322	1.743					0.045	0.964			0.049	1.738		2.360
Sum	3.002	3.992	4.009	3.003	4.031	3.986	24.001	24.001	16.127	15.592	3.002	24.002	3.009	4.018	20.106	3.993	3.001	4.013	20.043	15.664	24.001	19.946
mg	80.8	91.7	76.5	77.2	77.3		23.1	0.0	66.3	69.5	76.1	33.7	77.5	78.7	(An_{89})		73.8	77.9	(An_{83})	69.3	16.4	(Or_{61})

Ol – olivine, Cpx – clinopyroxene, Lc – leucite, Timt – titanomagnetite, Amp – amphibole, Sp – spinel, Plag – plagioclase, Mt – magnetite, San – sanidine, PC – phenocryst core, PR – phenocryst rim, G – groundmass phase, Inc – inclusion

* Fe_2O_3 calculated assuming stoichiometry

Table 2. Major and trace element data for the Batu Tara rocks

	Older extrusives (Group 1)						Dykes (Group 2)				(Group 3)
	B4155	67132	67130	67148	67127	B4150	67137	67147	67145	67146	B4200
SiO_2	48.77	47.76	47.68	48.14	49.74	48.71	48.05	46.43	45.68	45.68	53.28
TiO_2	0.82	0.90	0.90	0.93	0.78	0.87	0.94	1.16	1.17	1.29	0.65
Al_2O_3	12.17	13.48	13.58	13.76	15.68	14.50	15.98	16.07	16.49	17.95	18.55
Fe_2O_3	2.73	4.42	3.67	3.46	3.75	3.40	2.35	3.24	4.12	2.80	3.39
FeO	5.51	4.23	4.84	5.13	4.37	5.69	6.19	5.94	6.32	7.29	3.42
MnO	0.16	0.17	0.17	0.17	0.17	0.19	0.17	0.17	0.20	0.20	0.16
MgO	9.53	8.38	8.28	7.68	6.40	5.94	6.19	6.35	5.51	4.22	3.19
CaO	11.65	12.24	12.08	12.05	10.28	10.05	10.86	11.97	11.90	10.20	7.05
Na_2O	1.72	1.48	2.79	1.87	2.24	1.98	2.87	1.80	2.28	2.45	3.55
K_2O	5.09	4.69	3.42	4.51	4.97	6.71	3.65	4.18	4.02	4.75	5.20
P_2O_5	0.95	0.87	0.84	0.85	0.78	0.94	0.72	0.82	1.02	1.26	0.61
LoI	0.39	0.65	1.46	1.00	0.63	0.44	1.04	1.43	0.66	1.26	0.36
Total	99.49	99.27	99.71	99.55	99.79	99.42	99.01	99.56	99.37	99.35	99.41
M[a]	71.6	68.2	68.1	67.9	63.5	58.8	61.1	60.1	53.6	47.5	50.9
K_2O/Na_2O	2.96	3.17	1.22	2.41	2.22	3.38	1.27	2.32	1.76	1.94	1.46
Sc	36	36	37	42	32	30	34	35	30	16	18
V	268	276	302	307	278	282	300	338	392	346	184
Cr	461	287	272	244	194	120	91	98	53	10	13
Ni	105	81	79	68	51	43	38	32	27	18	15
Rb	266	196	184	192	206	288	164	215	159	158	175
Sr	793	819	818	847	940	1040	955	937	1155	1248	1016
Y	25	35	33	30	43	42	34	51	36	31	34
Zr	183	206	214	212	218	312	184	134	176	208	268
Nb	13	17	20	18	12	22	10	9	12	16	20
Ba	926	1128	1119	1072	1057	1256	1315	1177	1050	1513	1095
La	41.2	45.7	47.0	51	68.5	81.9	58.3	38.5	49.5	57.6	72.3
Ce	90.1	91.9	95.1	100	140.6	173	116.5	78.7	105.9	120	150
Pr	10.0	10.7	11.6		16.9		12.5	9.05	12.1	12.8	15.4
Nd	41.9	45.8	47.6	47	68.0	82	55.0	39.2	54.6	53.6	59.7
Sm	8.4	10.5	10.3		14.5	16.6	11.5	8.83	12.1	10.8	11.6
Eu	2.34	3.05	2.79		3.88	4.18	3.36	2.50	3.37	3.05	3.07
Gd	7.30	8.71	8.65		11.9	13.1	9.58	7.18	9.95	9.31	9.41
Dy	5.56	6.52	6.50		8.29	9.01	6.93	5.61	7.45	7.05	6.47
Er	2.52	3.01	2.86		3.64	3.58	3.10	2.42	3.54	3.38	3.23
Yb	1.96	2.40	2.29		2.78	2.68	2.45	2.11	2.76	3.00	2.98
Th		11.2	14.7	12.7						13.1	
Rb/Sr	0.335	0.239	0.225	0.227	0.219	0.277	0.172	0.230	0.138	0.127	0.172
K/Rb	159	199	154	195	200	193	185	161	210	250	247
$(La/Yb)_N$	13.9	12.6	13.6		16.3	20.2	15.7	12.1	11.8	12.7	16.0

[a] $100\ Mg/(Mg+Fe^{2+})$ based on $Fe_2O_3/FeO=0.20$

1985), and leucite basanites from the Eifel (Mertes and Schmincke 1985) and Italy (Baldridge et al. 1981). Experimental work by Foley (1985) showed that the Fe^{3+} contents of spinels and leucites in K-rich rocks decrease with decreasing fO_2 conditions during crystallization and that the relatively low Fe_2O_3 contents of the Gaussberg and Batu Tara leucite phenocrysts are consistent with crystallization at fO_2 close to the NNO buffer.

Plagioclase phenocrysts in the dyke rocks are very calcic (An_{93-82}; see Table 1 and Fig. 12) and display both normal and reverse zoning. Groundmass plagioclases in the dykes and lavas are more sodic (An_{78-47}).

Groundmass amphiboles are magnesian-hastingsites with $K_2O/Na_2O<1$ and relatively low TiO_2 contents. Rare groundmass biotites also have low Ti contents compared with similar groundmass phases in New South Wales leucitites (Cundari 1973), reflecting the relatively low whole-rock TiO_2 contents of the Batu Tara rocks.

A homogeneous titaniferous magnetite occurs as microphenocrysts and in the groundmass of all of the Batu Tara rocks, but ilmenite was not observed. The groundmass titanomagnetites generally are enriched in Ti and depleted in Mg, Al and Cr compared with coexisting phenocrysts. The relatively high Al contents of the phenocrysts, which is also a characteristic of titanomagnetite phenocrysts in the Italian leucite basanites, may be attributable to the relatively low silica activities of the crystallizing K-rich magmas (Baldridge et al. 1981). The increased Ti (ulvospinel) contents of the groundmass titanomagnetites compared with associated phenocrysts is probably due to lower fO_2 conditions resulting from cooling (Wilkinson and Stolz 1983).

Cr-rich spinel (Table 1) occurs as rare inclusions in olivine phenocrysts ($mg=76$) from leucite basanite 67148 (Table 2). Similar spinel inclusions in Mg-rich olivine phenocrysts from leucite lamproites have been interpreted as near-liquidus phases of primary melts (Foley 1985). Cr-rich spinels included in relatively Fe-rich olivines are more difficult to explain. Although the Batu Tara rock in which the Cr-spinel inclusions occur in olivine has an M-value (67) within the range generally accepted for primary melts of mantle peridotite with $mg \sim 89$, the low mg-values of the clino-

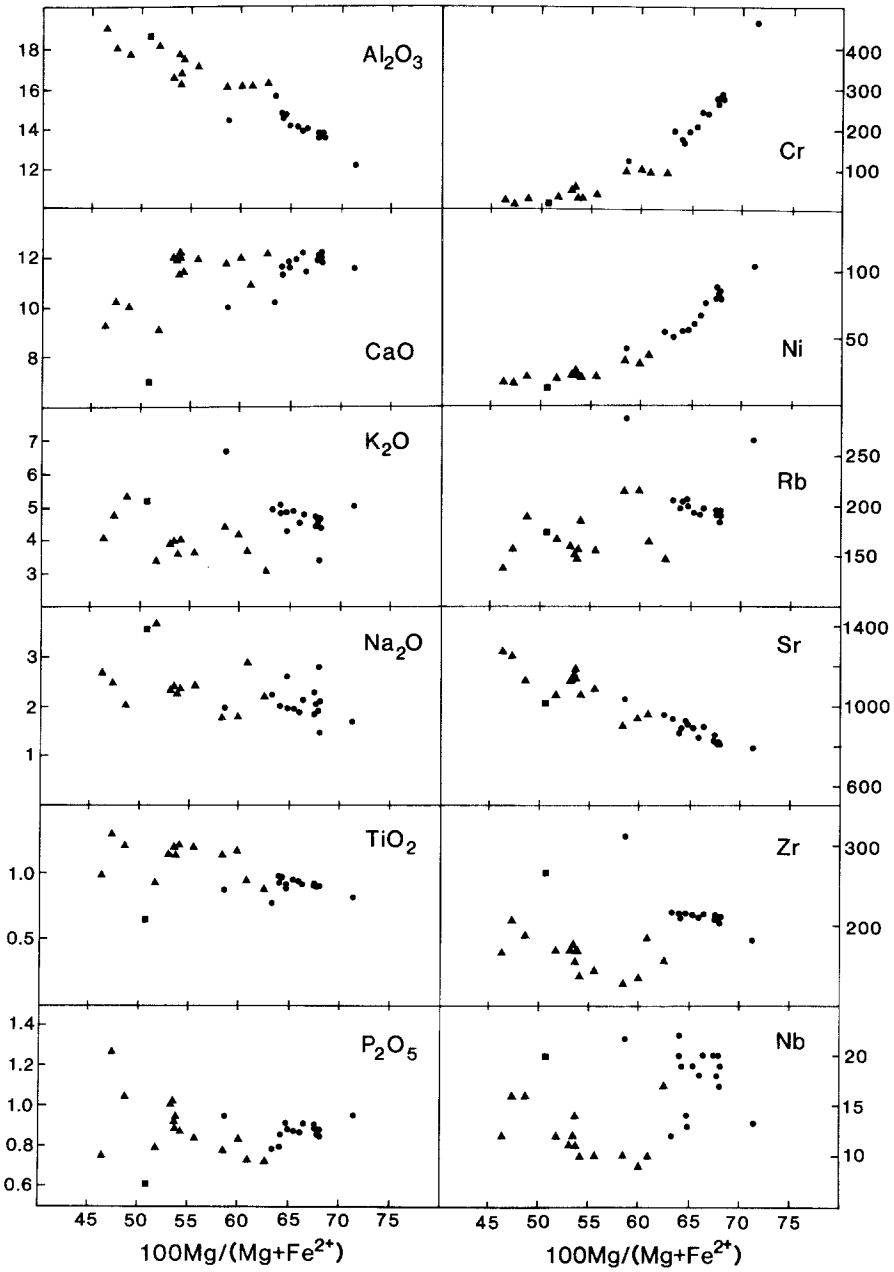

Fig. 5. Variation of several major and trace elements as functions of whole-rock 100 $Mg/(Mg+Fe^{2+})$ for the Batu Tara leucite basanite lavas (*dots*), dykes (*triangles*), and a biotite leucite tephrite (*square*)

pyroxene and olivine phenocrysts imply an unusually high value for $K_{D\,Fe-Mg}^{Ol-liq}$ (~ 0.48) if the rock represents a liquid composition (Roeder and Emslie 1970; Takahashi and Kushiro 1983).

Compositional data

Major and trace element data

Representative major and trace element analyses of the Batu Tara lavas and dykes are presented in Table 2. The analyses were performed by XRF on a Philips PW1410 spectrometer at the University of Tasmania following the methods of Norrish and Chappell (1977). REE analyses containing data for elements in addition to La and Ce were obtained either by using an ion-exchange XRF procedure (Robinson et al. 1986) or by isotope dilution at the University of Adelaide (B4150, Table 2). Precision for the XRF REE analyses is 1–4%, whereas the precision for the isotope dilution analyses is better than 1%. Accuracy was monitored by concomitant analysis of USGS standard rocks.

The petrographic and mineralogical differences between the lavas and dykes are reflected in their chemical compositions. The early eruptives (Group 1) generally are characterized by lower TiO_2, Al_2O_3, total FeO, Sr and V, and higher SiO_2, MgO, Rb, Zr, Nb, Ni and Cr, than the later (Group 2) dyke rocks. The limited chemical data for the biotite leucite tephrites (Group 3) indicate higher SiO_2, Na_2O, Zr, LREE and lower TiO_2, FeO, MgO, CaO, P_2O_5 and V than the other two groups. Although the three rock groups are chemically distinguishable, plots for several major and trace elements as functions of M-values (Fig. 5) indicate that many of the chemical differences are gradational between groups. If all analyzed specimens are regarded as a single suite, decreasing M values correlate with increasing Al_2O_3, FeO and Sr, and decreasing Rb, Sc, Cr and Ni. Coherent variations with M are not displayed by CaO, TiO_2, P_2O_5, Na_2O, K_2O, Y, Zr, Nb, Ba, LREE and K/Rb.

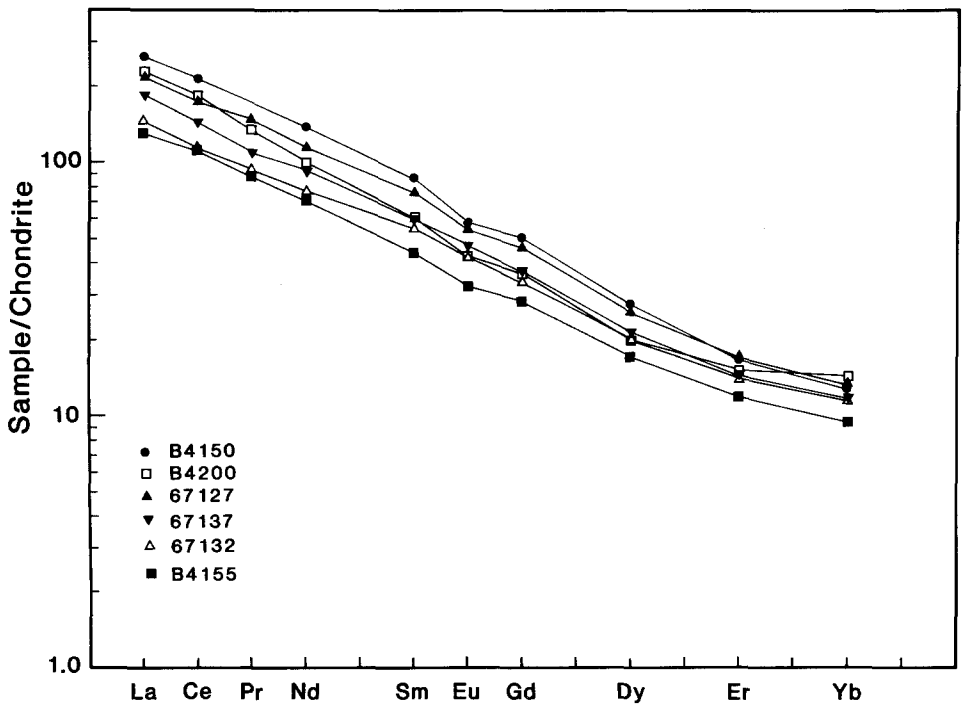

Fig. 6. Chondrite-normalized rare earth element plots for selected specimens which span the range of rare earth element concentrations in the Batu Tara leucite basanite and tephrite volcanics and dykes

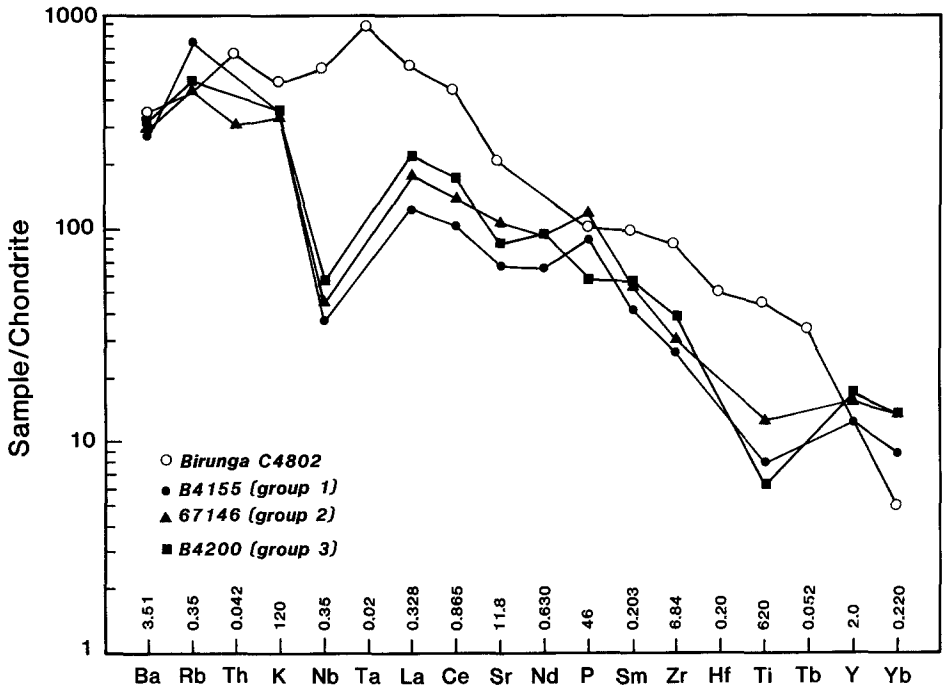

Fig. 7. Chondrite-normalized minor and trace element concentrations in selected K-rich volcanics from Batu Tara. The pattern for a K-rich eruptive from Birunga (*open circles*) (Mitchell and Bell 1976) is shown for comparison. Normalization factors shown on the x-axis are from Thompson (1982) except for Ba which is an estimate for 'undepleted' mantle from Sun (1980)

Chondrite-normalized REE plots for the Batu Tara rocks (Fig. 6) are straight near-parallel trends characterized by moderate LREE enrichment ($[La/Yb]_N = 12–20$) relative to chondrite (~100–200 X chondrite for La). Total REE concentrations tend to increase with decreasing M within the older lavas and within the dykes and younger lavas, but the trend is not continuous through the whole series and some of the more magnesian rocks have higher total REE than more 'evolved' variants. Very slight negative Eu anomalies are evident for several dykes and older lavas but there is no evidence of positive anomalies which might indicate plagioclase and, or, leucite accumulation, even though leucite is a common phenocryst phase in the lavas and both phases are common as phenocrysts in the dykes. However, assuming reasonable REE abundances for plagioclase (Stolz 1985) and leucite (Whitford 1975a), addition of approximately 20–30 wt. % plagioclase phenocrysts or greater than 40 wt. % leucite would be required before a positive Eu anomaly would be discernible.

The characteristic relative depletion of Ti, Nb and LREE in the Batu Tara leucite basanites compared with Foley et al.'s (1987) group II K-rich volcanics is evident in a chondrite-normalized plot (Fig. 7). In contrast, Zr does not appear to be relatively depleted in the Batu Tara rocks,

Table 3. Sr, Nd and O isotope data for the Batu Tara rocks

Sample	$^{87}Sr/^{86}Sr$	$^{143}Nd/^{144}Nd$	$\delta^{18}O$
B4155	0.70609±3	0.512578±20	6.31
67130	0.70571±1	0.512609±16	
67132	0.70571±1	0.512593±14	
B4150	0.70706±3	0.512447±20	6.50
67137	0.70605±1	0.512566±10	

although the alkali earth elements Ba and Sr display negative anomalies and P displays slight positive anomalies in the more primitive compositions.

Isotopic data

Sr and Nd isotopes for the Batu Tara rocks (Table 3) were determined by A.J.S. at the Department of Earth Sciences, University of Leeds and by G.A. Jenner at Abteilung Geochemie, Max-Planck Institut für Chemie, Mainz (Varne and Foden 1986; Jenner GA, White WM, Dupre BR, Foden JD, Kerrich R: Geochemistry of Quaternary volcanics from the East Sunda Arc, Indonesia: isotopic and incompatible element constraints on the nature of their source region, in prep.). At Leeds, Sr and Nd were separated from 100–150 mg of powdered sample using standard ion-exchange techniques and analysed as metal species on a VG Isomass 54E and Micromass 30, respectively. All Nd isotope ratios were normalized to $^{143}Nd/^{144}Nd = 0.7219$, and $^{143}Nd/^{144}Nd$ values were normalized to a value for BCR-1 of 0.51262. $^{87}Sr/^{86}Sr$ values were normalized to values of 0.70800 and 0.71023 on the Eimer and Amend and NBS987 standards, respectively.

The Sr and Nd isotope data for the Batu Tara rocks indicate that they are isotopically distinct from K-rich eruptives from Sumbawa (Whitford et al. 1978; Varne and Foden 1986), and Java (Whitford 1975a, b; Whitford et al. 1981). Indeed, several of the Batu Tara specimens have amongst the highest $^{87}Sr/^{86}Sr$ and lowest $^{143}Nd/^{144}Nd$ values of analyzed volcanics from the Sunda arc. There is also significant variation of $^{87}Sr/^{86}Sr$ and $^{143}Nd/^{144}Nd$ between these samples implying substantial isotopic heterogeneity in their source region. The Batu Tara isotopic data extend the negative correlation of $^{143}Nd/^{144}Nd$ with $^{87}Sr/^{86}Sr$ displayed by other volcanics from the Sunda arc (Fig. 8) which broadly coincides with the 'mantle array' (O'Nions et al. 1979; Zindler and Hart 1986). The $^{87}Sr/^{86}Sr$ values of recent calcalkaline volcanics from the Banda arc (Whitford et al. 1981) are even higher than those of the Batu Tara rocks (Fig. 8) although their $^{143}Nd/^{144}Nd$ values are comparable.

The $\delta^{18}O$ values for the Batu Tara rocks (6.3–6.5; R. Kerrich, pers. comm.) are within the range of unmodified mantle materials (James 1981) suggesting negligible contamination by continental crustal materials (Varne and Foden 1986).

Discussion

Low-pressure phase relations

When plotted in terms of the recalculated normative parameters of the simple system Fo–Ks–Qz (Fig. 9), the Batu Tara and similar K-rich rocks from Soromundi and Sangenges, Sumbawa (Foden and Varne 1980; Varne and Foden 1986) fall along reasonably well-defined olivine control lines. Although this is partly an artifact of the projection technique, these trends are consistent with the crystallization sequence inferred from phenocrysts, and the low-pressure (<2 kb) phase relations in the simple system (Luth 1967) which predict the early crystallization of olivine and clinopyroxene followed by leucite, and mica as a groundmass phase. The effect of clinopyroxene is ignored in this projection from diopside. However, in the normative projection Di–Ol–Ne (Fig. 10) the Batu Tara compositions plot close to the 1 bar (FMQ) olivine+plagioclase+clinopyroxene cotectic determined by experiments on a range of natural compositions (Sack et al. 1987), and they are displaced from the higher pressure olivine+orthopyroxene+clinopyroxene cotectic defined by more 'primitive' compositions. This suggests that the Batu Tara rocks are the result of crystal-liquid equilibration and fractionation processes at low pressures. In a normative Di–Ne–Or projection from olivine and leucite (Fig. 11) several of the relatively 'evolved' and phenocryst-poor dyke rocks plot

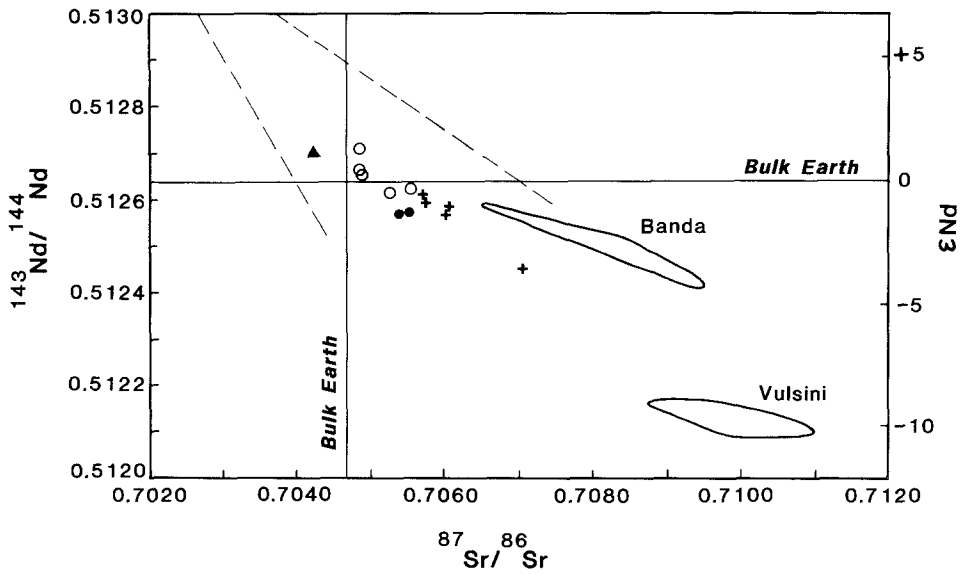

Fig. 8. Plot of $^{87}Sr/^{86}Sr$ versus $^{143}Nd/^{144}Nd$ for K-rich alkaline volcanics from the Sunda arc. Key: Batu Tara (*pluses*), Sangenges (*dots*), Soromundi (*open circles*), Muriah (*solid triangle*). The 'mantle array' defined by mid-ocean ridge and ocean island basalts, and fields for the Banda arc and Vulsini are shown for comparison

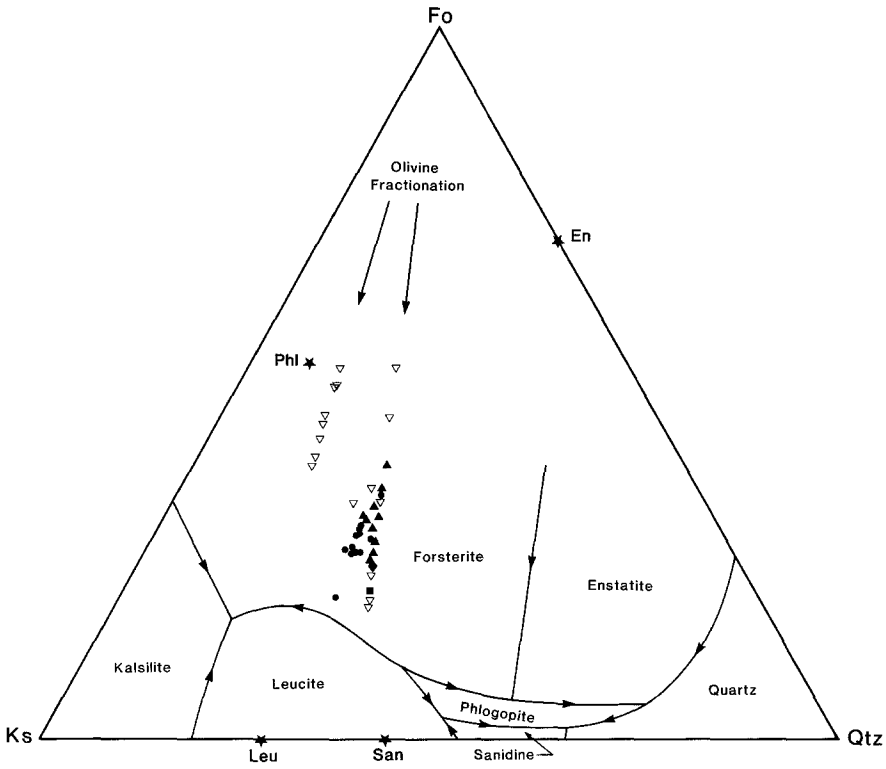

Fig. 9. Normative Fo–Ks–Qtz diagram showing the Sangenges, Soromundi (*open triangles*) and Batu Tara (Group 1 – *dots*, Group 2 – *solid triangles*, Group 3 – *square*, recalculated glass inclusion-*diamond*) compositions relative to the low-pressure ($PH_2O = 2$ kb) phase relations in the simple system after Luth (1967)

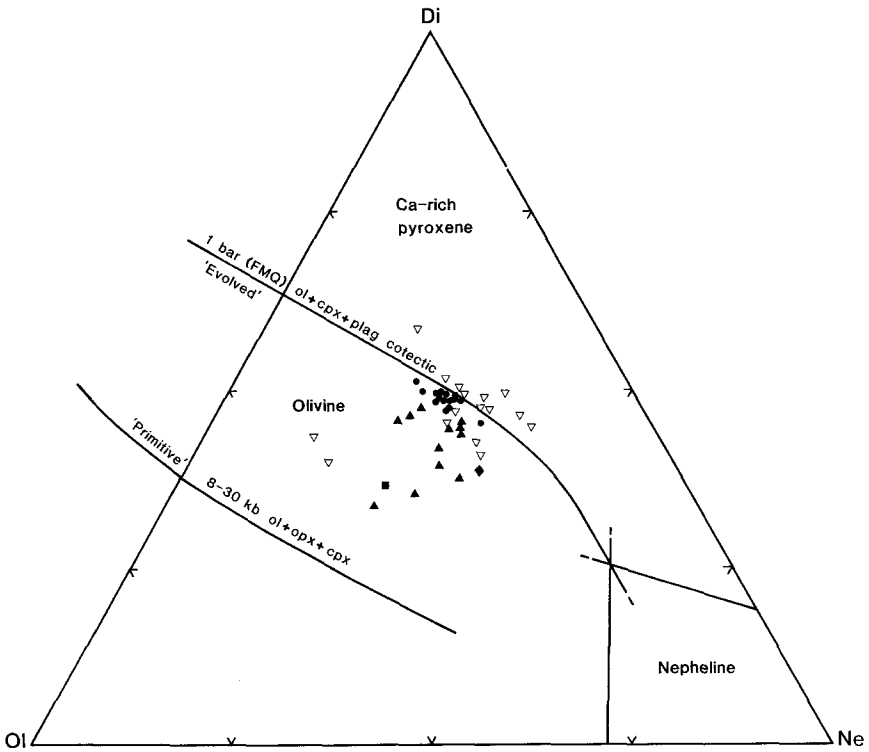

Fig. 10. Normative Di–Ol–Ne diagram showing the recalculated normative compositions of the Group 1, 2 and 3 Batu Tara rocks and similar K-rich rocks from Soromundi and Sangenges, Sumbawa. Symbols as for *Fig. 9*. The traces of the 1 bar (FMQ) olivine + clinopyroxene + plagioclase cotectic and the 8–30 kb olivine + orthopyroxene + clinopyroxene cotectic are from Sack et al. (1987)

close to the 1 bar (FMQ) olivine + leucite + plagioclase + clinopyroxene cotectic (Sack et al. 1987), whereas the Group 1 Batu Tara rocks with relatively high modal clinopyroxene are displaced from the cotectic toward the Di–Ne join. Leucitite and leucite basanite eruptives from Sumbawa (Foden and Varne 1980; Varne and Foden 1986) also display this trend of enrichment in normative Di and Ol which is consistent with the accumulation of variable quantities of clinopyroxene and olivine phenocrysts in these K-rich magmas.

Plagioclase and leucite are common felsic minerals of the Batu Tara rocks, sanidine is rare and nepheline is absent, despite its appearance in the CIPW norms. When the salic normative constituents of the Batu Tara leucite basan-

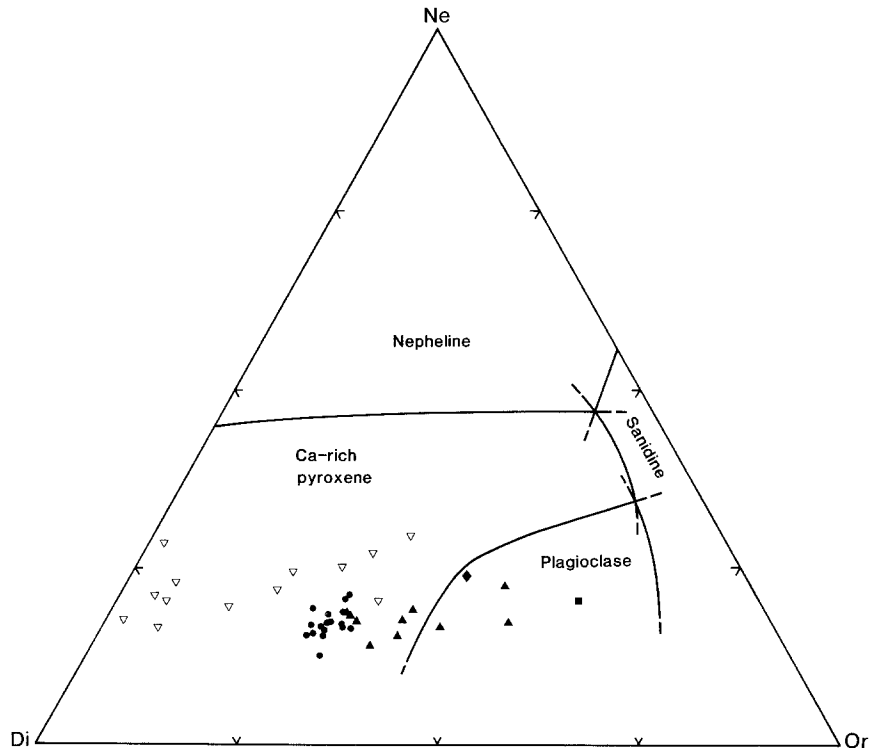

Fig. 11. Normative Di–Ne–Or diagram showing the recalculated normative compositions of the Batu Tara, Soromundi and Sangenges K-rich rocks. Symbols as for *Figs. 9* and *10*. The 1 bar cotectics are reproduced from Sack et al. (1987)

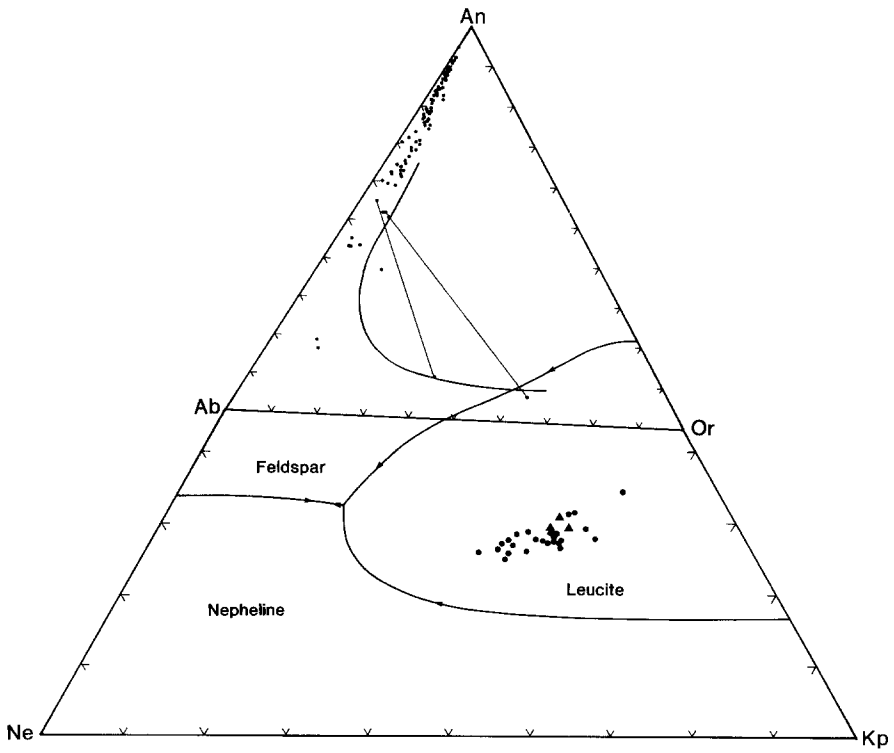

Fig. 12. Base of the phonolite pentahedron with the ternary feldspar plane rotated into the plane $NaAlSiO_4-KAlSiO_4-SiO_2$. The 1-bar experimental phase boundaries and the line marking the limit of ternary solid solution in the feldspar system are from Carmichael et al. (1974). Compositions of phenocryst and groundmass plagioclases and groundmass sanidines from the Batu Tara leucite basanites are represented by *dots* in the *upper part* of the diagram. The recalculated normative salic components of the Batu Tara and Italian leucite basanites are represented by *dots* and *triangles*, respectively, in the phonolite pentahedron. Tie-lines join coexisting groundmass plagioclase and sanidine compositions

ites are projected into the 'phonolite pentahedron' of Carmichael et al. (1974), they fall near the leucite-plagioclase join in a similar position to leucite basanites from the Roman province and Vesuvius, Italy (Fig. 12).

Baldridge et al. (1981) showed that the felsic mineral groundmass assemblages of these Italian leucite basanites include either plagioclase + leucite ± sanidine or plagioclase + leucite + sodalite, and accessory biotite ± hastingsitic amphibole. They also pointed out that the felsic mineralogy of the rocks was in reasonable accordance with the equilibrium assemblages predicted from the likely low-pressure phase relations within the pentahedron and with their normative compositions, but argued that the presence and nature of volatile constituents could influence the groundmass

paragenesis. They proposed that the presence of chlorine might cause sodalite to appear in lieu of nepheline, and that the presence of fluorine could lead to the appearance of phlogopite at the expense of sanidine according to the reaction proposed by Brown and Carmichael (1969):

$KMg_3AlSi_3O_{10}F_2 + 3/2\ SiO_2 = 3/2\ Mg_2SiO_4 +$
biotite liquid olivine
$KAlSi_3O_8 + F_2$
sanidine

Neither sodalite nor nepheline has been found, as yet, in the Batu Tara leucite basanites and sanidine has only been observed in the groundmass of two leucite tephrites. The phase relations in Fig. 11 indicate that relatively dry melts crystallizing on the olivine + clinopyroxene + plagioclase + leucite cotectic which did not become saturated in sanidine would not be expected to have precipitated nepheline. However, where both biotite and a hastingsitic amphibole occur as groundmass phases, we speculate that just as the presence of fluorine could favour the appearance of phlogopite in place of sanidine (Baldridge et al. 1981), so the presence of hydroxyl in the melt might have inhibited the appearance of modal nepheline by causing amphibole to crystallize, by analogy with the known reaction:

$NaCa_2Mg_4AlAl_2Si_6O_{22}(OH)_2 = 3CaMgSi_2O_6 +$
amphibole clinopyroxene
$2Mg_2SiO_4 + 2NaAlSiO_4 + MgAl_2O_4 + CaAl_2Si_2O_8 + H_2O$
olivine nepheline spinel plagioclase

Primary magmas and crystal fractionation/ accumulation

If the Batu Tara rocks were to be considered as a single suite, the gradational trends of some major and trace elements (Fig. 5) could be interpreted as indicating a genetic relationship between these rocks. Progressive decreases in Cr and Ni with decreasing M-values (and also with order of eruption or emplacement) could be due to fractionation of olivine and clinopyroxene from a parental leucite basanite melt.

However, although variations of Ni and Cr with M are in keeping with a cogenetic model, coupled variations of several trace elements, e.g. Cr vs Zr and Ni vs Rb (Fig. 13a and b), are not easy to explain as a result of simple closed-system fractionation of the observed phenocrysts from a single parental magma. In plots of highly incompatible elements against compatible elements, fractionation of olivine and clinopyroxene should generate smoothly curving variation trends, whereas mixing will produce straight-line variation trends. The data in Fig. 13a and b do not fall on a single fractionation or mixing trend, suggesting that several magmas with different incompatible trace element contents were involved. These may have been 'primitive' magmas which evolved along separate liquid lines of descent, or relatively 'evolved' magmas which accumulated varying amounts of clinopyroxene, olivine and leucite phenocrysts.

Before useful quantitative modelling of fractionation processes can be undertaken, it is necessary to identify any likely potential parental magma or magmas. Primitive magmas are commonly assumed to have been in equilibrium with residual mantle olivine of $mg = 88$–90 (Irving and

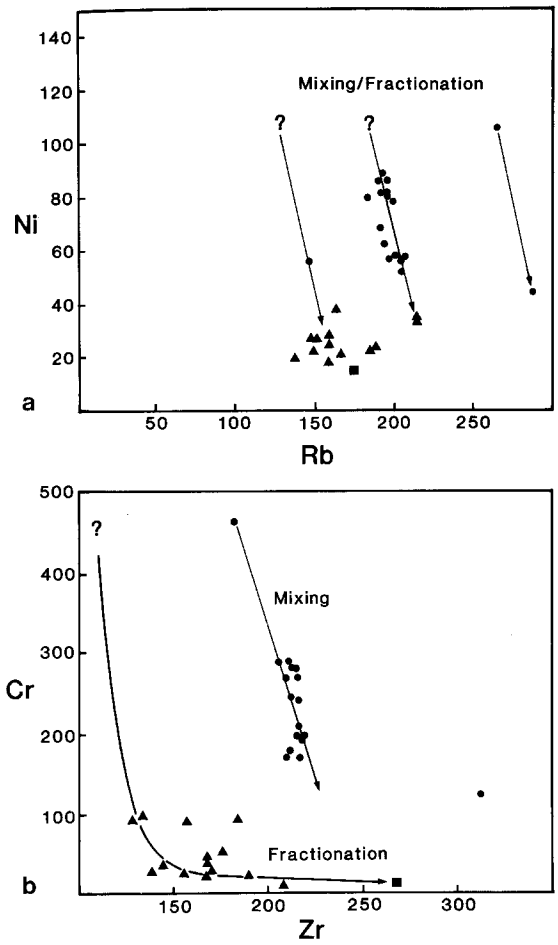

Fig. 13a, b. Plots of **a** Ni versus Rb and **b** Cr versus Zr for the Batu Tara rocks indicating the existence of several discrete suites and mixing or fractionation trends. Symbols as for *Fig. 9*

Green 1976), and are characterized by high concentrations of Ni (>200–250 ppm) and Cr (>250–300 ppm). However, very few arc volcanics (including Mg-rich types) have Ni contents in this range (Perfit et al. 1980).

M-values for the Batu Tara volcanics (Table 2) were calculated with $Fe_2O_3/FeO = 0.2$, as this value is commonly used for intraplate alkaline basaltic volcanics. This value may be too low for the Batu Tara rocks which have measured Fe_2O_3/FeO ratios of at least 0.4, although they may have been increased by oxidation during or after eruption. The maximum calculated M-value (72) falls in the range of 'primitive' melts and, together with the high Cr and relatively high Ni contents of this rock, could support its classification as a primary composition and potential parent for the early lava suite. However, as the Batu Tara volcanics are porphyritic it is important to evaluate the extent to which the analyzed rocks could represent melt compositions and the extent to which their compositions may have been modified by phenocryst accumulation.

Assuming $K_{D\,Fe-Mg}^{Ol-liq} \sim 0.30$ (Roeder and Emslie 1970; Takahashi and Kushiro 1983), if the bulk-rock composition of B4155 ($M = 72$) were to have been a liquid, its liquidus olivine would have been $mg \sim 89.5$. Examination of Fig. 3, which shows mg-values of olivine and clinopyroxene phenocrysts as a function of the host M-value, indicates that the olivine (and clinopyroxene) phenocrysts in the most

magnesian eruptive compositions seem too Fe-rich to be liquidus phases of their hosts. The restricted range of olivine core compositions over a wide range of whole-rock M-values strongly suggests that much of the chemical variation displayed by the Batu Tara rocks is a function of variable degrees of phenocryst accumulation in a common melt or melts of similar M.

The M-value of this hypothetical melt can be estimated by consideration of the most magnesian olivine phenocrysts. M-values of approximately 47–51 are appropriate for olivine phenocrysts with $mg = 74$–78. This calculation is, of course, sensitive to the choice of the Fe_2O_3/FeO value for the melt; higher melt Fe_2O_3/FeO values will result in more magnesian liquidus olivines for bulk compositions of a particular M.

Glass inclusions trapped in phenocrysts provide an additional method of estimating the composition of the melt from which they crystallized. It is important to bear in mind, though, that the melt trapped by the growing phenocrysts will be slightly more evolved than the liquidus melt simply due to crystallization of the early phenocrysts. Other factors which need to be considered when evaluating glass inclusions as a guide to melt compositions include the effects on the melt composition of the continued crystallization of the host phase on the walls of the melt inclusion, the possibility of subsolidus differential diffusion or cation exchange between glass and enclosing crystal, and the possibility that the melt which was trapped was from a nucleation zone, adjacent to a phenocryst, characterized by concentration gradients (Anderson 1979; Gill 1981). The effects of these processes can be minimized by examining relatively large glass inclusions (>30 μm, Anderson 1979) in phenocrysts of varying composition.

In this study, glass inclusions (~ 50 μm) from olivine, clinopyroxene and leucite phenocrysts in leucite basanite 67148 were analyzed. A best estimate for the initial melt composition was achieved by adding varying quantities of each enclosing phase to the compositions of the trapped glasses until reasonable convergence between the adjusted glass compositions was achieved. Average compositions of the glasses, and of the estimated original melt composition prior to modification by continued growth of the enclosing crystals are presented in Table 4 together with average groundmass scans from several porphyritic rocks. Several of the dyke rocks (e.g. 67146, Table 2) have compositions which resemble the recalculated glass composition. Their low M-values (~ 48) and low Cr and Ni contents indicate they are unlikely to have been primary melts of mantle peridotite.

Assuming that the olivine phenocrysts enclosing the glass inclusions were in equilibrium with the melt, and that $K_D{}^{Ol-liq}_{Fe-Mg} = 0.30$ (Roeder and Emslie 1970; Takahashi and Kushiro 1983) the Fe_2O_3/FeO of the melt was calculated from the relation $K_D = (Fe^{2+}/Mg)_{Ol}/(Fe^{2+}/Mg)_{liq}$. This Fe_2O_3/FeO value (0.27) is lower than all the analysed whole-rock values suggesting that some post-eruptive oxidation of the Batu Tara rocks has occurred. Using equation 9 of Sack et al. (1980) and a liquidus temperature of 1,140° C estimated from Fig. 5 of Sack et al. (1987), the calculated $\log fO_2$ (-8.6) indicates melt temperature-fO_2 conditions appropriate to the NNO buffer. This suggests crystallization of the Batu Tara magmas under more oxidizing conditions than those commonly deduced for intraplate volcanics (i.e. FMQ; Stolz 1986), but less oxidizing than those deduced for K-rich volcanics from the Leucite Hills, Wyoming (Foley 1985).

Crystal-liquid equilibria

In addition to the appearance of leucite rims on clinopyroxene and olivine (Fig. 2b) which may be due to crystal-liquid disequilibria, the compositions of some phenocrysts are unlike those that would be expected from their whole-rock compositions. Cr-diopside cores and oscillatory zones in clinopyroxene phenocrysts (Figs. 2a and 4) are fairly common in the eastern Sunda volcanics (Foden and Varne 1980; Foden 1986) and in other K-rich volcanics and cumulate xenoliths (Barton et al. 1982; Conrad and Kay 1984). Zoned clinopyroxene phenocrysts are most abundant in the Group 1 Batu Tara rocks, but also occur in some Group 2 rocks. The systematic compositional differences between adjacent zones of the oscillatory-zoned phenocrysts may be explained by coupled $Fe^{2+} \rightleftarrows Mg^{2+}$ and $TiAl_2 \rightleftarrows MgSi_2$ exchange reactions between clinopyroxenes and silicate melts (Sack and Carmichael 1984). However, rapid and marked changes in melt composition or physical conditions in the melt seem necessary to promote these exchange reactions.

Similar zoning in pyroxenes from gabbroic xenoliths from Adak Island andesites (Conrad and Kay 1984) has been explained in terms of an open-system, periodically replenished magma chamber, but this explanation does not account for the sharp compositional boundaries between zones, or the absence of gradual normal or reverse zoning within individual zones.

In particular, mixing of magmas with strongly contrasting M-values, each with its crop of suspended clinopyroxene phenocrysts, initially should result in partial resorption of the relatively low-mg phenocrysts from the cooler, more Fe-rich magma, following their mixing with hotter, more Mg-rich magma. Such resorption features are occasionally observed in Batu Tara clinopyroxene phenocrysts on the outer margins of relatively Fe-rich zones in contact with more Mg-rich zones. Following mixing, fractional crystallization of the relatively Mg-rich magma should produce normal zoning in the precipitating clinopyroxene from Mg- and Cr-rich zones to more Fe-rich and Cr-poor compositions until the chamber is recharged with another batch of more primitive magma. We have observed that within individual crystals displaying cyclic zoning, the repeated relatively Fe-rich zones have remarkably similar mg-values. The periodic magma replenishment can only explain this regular zoning if the magma chamber were recharged consistently at the point when the mixed magma was crystallizing pyroxene of a specific, relatively Fe-rich composition. Although such regularity in recharging of the magma chamber is possible, it seems unlikely, as it also requires regularity in the rate of differentiation of the mixed magmas. In addition, large scale magma mixing is not supported by the observation that the oscillatory zoning is present only in some of the clinopyroxene phenocrysts within any particular rock.

Such restricted cyclic zoning is more likely to have occurred if magmas with contrasting M-values coexisted in a common magma chamber but remained in separate convecting cells, perhaps due to temperature, compositional and density differences (Huppert and Sparks 1984). Limited interaction along the interface between the convecting clino-

Table 4. Compositions of glass inclusions and groundmasses

	1	2	3	4	5	6	7	8	9
SiO_2	48.79	48.44	48.29	48.81	48.05	48.46	48.44	48.78	56.81
TiO_2	1.19	1.15	1.30	1.12	1.13	1.22	1.16	1.19	0.44
Al_2O_3	17.70	17.63	16.89	17.08	17.36	17.14	17.19	17.95	18.18
FeO #	9.62	9.56	10.00	9.55	9.62	9.40	9.52	9.49	4.09
MgO	3.68	3.74	4.39	4.13	4.07	4.12	4.11	4.06	1.07
CaO	8.08	9.14	9.43	8.77	9.00	8.84	8.87	9.21	3.74
Na_2O	3.32	3.40	3.46	3.17	3.35	3.28	3.27	3.54	4.20
K_2O	5.25	5.27	4.18	5.00	5.19	5.06	5.08	4.27	6.73
P_2O_5	1.30	1.26	1.42	1.24	1.24	1.33	1.27	1.37	0.35
Total	98.93	99.59	99.36	98.87	99.01	98.85	98.91	99.86	95.61
mg	40.5	41.1	43.9	43.5	43.0	43.9	43.5	43.3	31.8

1–3. Glass inclusions in clinopyroxene, olivine and leucite, from 67148.
4. Analysis 1 + 5% clinopyroxene. 5. Analysis 2 + 1% olivine.
6. Analysis 3 + 6% leucite. 7. Average of analyses 4–6.
8. Groundmass scan of 67148. 9. Groundmass scan of 67130.

FeO # = Total Fe as FeO; $mg = 100\ Mg/(Mg + \sum Fe)$

pyroxene phenocryst-bearing magma bodies could result in the transfer of a small volume of melt and phenocrysts between these cells without the need for mixing of large quantities of magma and extensive crystallization. This could explain the lack of compositional change within zones, the presence of some unzoned crystals, the Cr-diopside cores in some phenocrysts and relatively Fe-rich cores in others, and the sharp boundaries between zones which would result from incorporation and rapid mixing of a relatively small volume of melt and crystals with the contrasting magma. Phenocrysts without oscillatory zoning are inferred to have avoided the mixing zone. Cr-spinel inclusions in relatively Fe-rich olivine phenocrysts (e.g. Table 1, No. 67148) may have precipitated together with the Cr-diopside cores and oscillatory zones from more Mg-rich and Cr-rich magmas.

The restricted range of olivine compositions (Fig. 3) and the absence of similar oscillatory zoning (or in fact any zoning) in the olivine and in some of the more Fe-rich clinopyroxene phenocrysts could imply that the olivine and some of the clinopyroxene have reequilibrated with a relatively Fe-rich liquid due to Fe–Mg diffusion through the lattice. Although the diffusion coefficients for Fe–Mg in olivine indicate that compositional homogenization of phenocrysts could be achieved in a relatively short time, Fe–Mg diffusion coefficients for clinopyroxene are an order of magnitude smaller (Lasaga 1983). Depending on which diffusion coefficients are adopted, the period required for reequilibration of the clinopyroxene phenocrysts could be as short as a few hundred years or as long as a million years. The oscillatory-zoned clinopyroxene phenocrysts may also have undergone some crystal-liquid reequilibration, as pyroxene phenocrysts from all of the rocks examined have relatively Fe-rich rim compositions, indicating residence in relatively Fe-rich melt immediately prior to eruption. If so, the absence of Fe–Mg zoning within individual zones of these oscillatory-zoned clinopyroxenes could be due to Fe–Mg diffusion, whereas there was minimal exchange between adjacent zones, probably due to the complex nature of the substitutions in the Cr-rich and Cr-poor compositions.

Calculated effects of crystal accumulation on bulk composition

There is considerable evidence which suggests that most Batu Tara whole-rock compositions were produced at low pressures by redistribution and accumulation of varying amounts of phenocrysts in relatively 'evolved' magmas. The significant differences in the concentrations of incompatible trace elements between the Group 1 and 2 Batu Tara rocks (Fig. 13) indicate that these groups cannot be related either by fractional crystallization or crystal accumulation processes, and that several 'evolved' magmas were involved. We have tested this possibility in a series of least squares mixing calculations which employ the recalculated glass composition (Table 4, analysis 7) as the melt composition for the Group 1 rocks and the composition of a near-aphyric dyke (Table 2, 67146) as the melt composition for the Group 2 rocks. These calculations (Table 5) indicate that the major element compositions of most Group 1 and Group 2 rocks can be explained by addition of varying quantities of olivine, clinopyroxene, leucite ± plagioclase to these proposed melt compositions. An exception to this in the Group 1 suite is provided by samples 67132 and 67130 (Table 2) which have almost identical major and trace element compositions yet their Na_2O/K_2O values are very different. Least squares calculations (Table 5) suggest that these two compositions could be generated from the same melt composition if substantial clinopyroxene and leucite were added to produce 67132 and if clinopyroxene were added and leucite were fractionated to produce 67130. If $K_{D\,Rb}^{Lc-liq} \sim 4$–5 (Cundari 1973), the addition or removal of leucite from a common melt should result in marked differences in the Rb contents of the derivatives. However, 67132 and 67130 have K/Rb of 199 and 154 respectively, and very similar Rb contents.

Mass-balance calculations (Table 5) also suggest that compositions such as biotite leucite tephrite B4200 (Group 3), which are chemically more 'evolved' than both proposed melt compositions, may have been produced by fractionation of one of these compositions.

If the observed range of compositions was produced

Table 5. Least squares mixing solutions for crystal accumulation and fractionation models

Sample		Melt[a]	Oliv	Cpx	Leuc	Plag	Timt	Apat	$\sum r^2$
Group 1									
B4155		47.0	8.5	32.4	12.8		−1.0	0.3	0.262
67132		53.5	4.4	31.2	10.3			0.6	0.479
67130		77.1	5.5	22.0	−2.6		−2.4	0.4	0.434
67148		60.6	3.1	28.1	7.6			0.6	0.436
67127		79.8	2.4	15.9	5.1		−2.3	−0.9	0.479
B4150		54.0	1.2	24.4	18.7		2.0	−0.3	0.655
Group 2									
67137		96.0	3.3	8.7	−3.5		−4.5		3.973
67147		71.7	1.4	19.9	3.8	4.2		−1.0	0.376
67145		83.2	−0.7	15.2	−0.1	2.0	1.2	−0.8	0.533
Group 3									
B4200	(76.8)	100.0	−0.9	−6.7	−4.9	−2.0	−5.9	−2.8	0.646

[a] The melt composition used for Group 1 and 3 rocks is the average recalculated glass composition (*Table 4*, analysis 7). The melt composition used for the Group 2 rocks is of a phenocryst-poor dyke (*Table 2*, 67146). The compositions of phenocrysts in 67127 and 67146 (Table 1) were used in calculations involving Groups 1 and 3, and Group 2 rocks, respectively

$\sum r^2$ = sum of the squares of the residuals

by accumulation of liquidus phases in relatively 'evolved' magmas, then it seems necessary to infer that these magmas were derived from several primary magmas, none of which are represented in the material collected. Low-pressure fractional crystallization of these primary magmas may have generated the relatively 'evolved' compositions which then underwent further intratelluric crystallization before they were erupted carrying varying quantities of accumulated phenocrysts.

The absence from our collection of any rocks which might represent primary magma compositions may be a sampling problem, as the rocks which crop out on the island of Batu Tara are a guide only to the most recent stages in the constructional and compositional evolution of the volcano.

Conclusions

Leucite basanite and leucite tephrite eruptives and dykes from the Batu Tara volcano, eastern Sunda arc, have minor and trace element characteristics (such as their strong enrichment in LIL and LRE elements, and relative depletion of Nb and Ti in chondrite-normalized plots) which are comparable with other alkaline volcanics of the Sunda Arc.

Combined mineralogical, isotopic and whole-rock compositional data for the Batu Tara leucite basanites indicate a complex genetic history which involved the accumulation of varying quantities of intratelluric precipitates in relatively 'evolved' melts at low pressures. The composition of one of these melts was estimated from the compositions of glass inclusions in phenocrysts of olivine, clinopyroxene and leucite. Trace element and Sr and Nd isotopic data indicate that several other relatively 'evolved' melts were also involved and that these were probably derived from several compositionally distinct parental leucite basanite magmas by low-pressure fractional crystallization of olivine, clinopyroxene and spinel.

Magnesian ($mg \sim 90$) and Cr-rich zones in complex oscillatory-zoned clinopyroxene phenocrysts provide indirect evidence that these more primitive magmas exist in high-level magma chambers beneath the volcano together with the relatively 'evolved' melts. The zoning is considered to be due to limited mixing of magmas and phenocrysts with markedly different M-values along an interface between discrete convecting magma bodies.

Acknowledgments. This research is part of a regional study of young volcanic rocks in the eastern Sunda arc funded by the Australian Research Grants Scheme and the University of Tasmania. Field work in Indonesia was approved by the Foreign Scholars Division of the Indonesian Institute of Sciences and sponsored by the University of Gadjah Mada. G.A. Jenner and R. Kerrich kindly allowed us to use unpublished isotopic data. P. Robinson and W. Jablonski provided assistance with XRF and microprobe analyses, respectively.

References

Anderson AT (1979) Water in some hypersthenic magmas. J Geol 87:509–531

Baldridge WS, Carmichael ISE, Albee AL (1981) Crystallization paths of leucite-bearing lavas: examples from Italy. Contrib Mineral Petrol 76:321–335

Barton M, Varekamp JC, van Bergen MJ (1982) Complex zoning of clinopyroxenes in the lavas of Vulsini, Latium, Italy: evidence for magma mixing. J Volcanol Geotherm Res 14:361–388

Ben Avraham Z, Emery KO (1973) Structural framework of the Sunda shelf. Bull Am Assoc Petrol Geol 57:2323–2366

Brouwer HA (1940) Geological and petrological investigations of alkali and calc-alkali rocks of the islands Adonara, Lomblen and Batoe Tara. In: Geological Expedition of the University of Amsterdam to the Lesser Sunda Islands, 2:1–94

Brown FH, Carmichael ISE (1969) Quaternary volcanoes of the Lake Rudolf Region: pt 1, the basanite-tephrite series of the Korath Range. Lithos 2:239–260

Carmichael ISE, Turner FJ, Verhoogen J (1974) Igneous Petrology. McGraw-Hill, New York, p 739

Conrad WK, Kay RW (1984) Ultramafic and mafic inclusions from Adak Island: crystallization history, and implications for the nature of primary magmas and crustal evolution in the Aleutian arc. J Petrol 25:88–125

Cox KG, Hawkesworth CJ, O'Nions RK, Appleton JD (1976) Isotopic evidence for the derivation of some Roman region volcanics from anomalously enriched mantle. Contrib Mineral Petrol 56:173–180

Cundari A (1973) Petrology of the leucite-bearing lavas in New South Wales. J Geol Soc Aust 20:465–492

Cundari A (1980) Role of subduction in the genesis of leucite-bearing rocks. Facts or fashion. Contrib Mineral Petrol 73:432–434

Curray JR, Shor GG, Raitt RW, Henry M (1977) Seismic refraction and reflection studies of crustal structure of the eastern Sunda and western Banda arcs. J Geophys Res 82:2479–2489

Dal Negro A, Carbonin S, Salviulo G, Piccirillo EM, Cundari A (1985) Crystal chemistry and site configuration of the clinopyroxene from leucite-bearing rocks and related genetic significance: the Sabatini lavas, Roman region, Italy. J Petrol 26:1027–1040

Dal Negro A, Cundari A, Piccirillo EM, Molin GM, Uliana D (1986) Distinctive crystal chemistry and site configuration of the clinopyroxene from alkali basaltic rocks: the Nyambeni clinopyroxene suite, Kenya. Contrib Mineral Petrol 92:35–43

Edgar AD (1980) Role of subduction in the genesis of leucite-bearing rocks: Discussion. Contrib Mineral Petrol 73:429–431

Foden JD (1986) The petrology of Tambora Volcano, Indonesia: A model for the 1815 eruption. J Volcanol Geotherm Res 27:1–41

Foden JD, Varne R (1980) Petrogenetic and tectonic implications of near coeval calc-alkaline to highly alkaline volcanism on Lombok and Sumbawa Islands in the eastern Sunda arc. In: Barber AJ, Wiryosujono S (eds) The Geology and Tectonics of Eastern Indonesia. Geological Research and Development Centre, Spec. Publ. 2:135–152

Foley SF (1985) The oxidation state of lamproitic magmas. Tschermaks Mineral Petrog Mitt 34:217–238

Foley SF, Venturelli G, Green DH, Toscani L (1987) The ultrapotassic rocks: Characteristics, classification, and constraints for petrogenetic models. Earth Sci Rev 24:81–134

Gill JB (1981) Orogenic Andesites and Plate Tectonics. Springer, Berlin Heidelberg New York, p 390

Hawkesworth CJ, Vollmer R (1979) Crustal contamination versus enriched mantle: $^{143}Nd/^{144}Nd$ and $^{87}Sr/^{86}Sr$ evidence from the Italian volcanics. Contrib Mineral Petrol 69:151–165

Holm PM, Lou S, Nielsen A (1982) The geochemistry and petrogenesis of the lavas of the Vulsinian district, Roman Province, Central Italy. Contrib Mineral Petrol 80:367–378

Huppert HE, Sparks RSJ (1984) Double-diffusive convection due to crystallization in magmas. Ann Rev Earth Planet Sci 12:11–37

Irving AJ, Green DH (1976) Geochemistry and petrogenesis of the Newer Basalts of Victoria and South Australia. J Geol Soc Aust 23:45–66

James DE (1981) The combined use of oxygen and radiogenic isotopes as indicators of crustal contamination. Ann Rev Earth Planet Sci 9:311–344

Jaques AL, Lewis JD, Smith CB, Gregory GP, Ferguson J, Chappell BW, McCulloch MT (1984) The diamond-bearing ultrapotassic (lamproitic) rocks of the West Kimberley region, Western Australia. In: Kornprobst J (ed) Kimberlites I: kimberlites and related rocks. Elsevier, Amsterdam, pp 225–254

Kuehner SM, Edgar AD, Arima M (1981) Petrogenesis of the ultrapotassic rocks from the Leucite Hills, Wyoming. Am Mineral 66:663–677

Lasaga AC (1983) Geospeedometry: an extension of geothermometry. In: Saxena SK (ed) Kinetics and Equilibrium in Mineral Reactions. Springer, Berlin Heidelberg New York, pp 81–114

Luth WC (1967) Studies in the system $KAlSiO_4-Mg_2SiO_4-SiO_2-H_2O$. I. Inferred phase relations and petrologic applications. J Petrol 8:372–416

Mertes H, Schmincke HU (1985) Mafic potassic lavas of the Quaternary West Eifel volcanic field. Contrib Mineral Petrol 89:330–345

Mitchell RH, Bell K (1976) Rare earth element geochemistry of potassic lavas from the Birunga and Toro-Ankole regions of Uganda, Africa. Contrib Mineral Petrol 58:293–303

Nicholls IA, Whitford DJ (1983) Potassium-rich volcanic rocks of the Muriah complex, Java, Indonesia: products of multiple magma sources? J Volcanol Geotherm Res 18:337–359

Nixon P, Thirlwall MF, Buckley F, Davies CJ (1984) Spanish and Western Australian lamproites: aspects of whole rock geochemistry. In: Kornprobst J (ed) Kimberlites I: Kimberlites and Related Rocks. Elsevier, Amsterdam, pp 285–296

Norrish K, Chappel BW (1977) X-ray fluorescence spectrometry. In: Zussman J (ed) Physical Methods in Determinative Mineralogy (2nd ed). Academic Press, London, pp 201–272

O'Nions RK, Carter SR, Evensen NM, Hamilton PJ (1979) Geochemical and cosmochemical applications of Nd isotope analysis. Ann Rev Earth Planet Sci 7:11–38

Pearce JA, Cann JR (1973) Tectonic setting of volcanic rocks determined using trace element analyses. Earth Planet Sci Lett 19:290–300

Perfit MR, Gust DA, Bence AE, Arculus RJ, Taylor SR (1980) Chemical characteristics of island arc basalts: implications for mantle sources. Chem Geol 30:227–256

Poli G, Frey FA, Ferrara G (1984) Geochemical characteristics of the South Tuscany (Italy) Volcanic Province: constraints on lava petrogenesis. Chem Geol 43:203–221

Robinson P, Higgins NC, Jenner GA (1986) Determination of rare-earth elements, yttrium and scandium in rocks by an ion exchange-X-ray fluorescence technique. Chem Geol 55:121–137

Roeder PL, Emslie RF (1970) Olivine-liquid equilibria. Contrib Mineral Petrol 29:275–289

Rogers NW, Hawkesworth CJ, Parker RJ, Marsh JS (1985) The geochemistry of potassic lavas from Vulsini, central Italy and implications for mantle enrichment processes beneath the Roman region. Contrib Mineral Petrol 90:244–257

Sack RO, Carmichael ISE (1984) $Fe^{2+} \rightleftarrows Mg^{2+}$ and $TiAl_2 \rightleftarrows MgSi_2$ exchange reactions between clinopyroxenes and silicate melts. Contrib Mineral Petrol 90:244–257

Sack RO, Walker DA, Carmichael ISE (1987) Experimental petrology of alkalic lavas: constraints on cotectics of multiple saturation in natural basic liquids. Contrib Mineral Petrol 96:1–23

Sack RO, Carmichael ISE, Rivers M, Ghiorso MS (1980) Ferric-ferrous equilibria in natural silicate liquids at 1 bar. Contrib Mineral Petrol 75:369–376

Sheraton JW, Cundari A (1980) Leucitites from Gaussberg, Antarctica. Contrib Mineral Petrol 71:417–427

Sorensen H (1974) The Alkaline Rocks. John Wiley and Sons, London

Stolz AJ (1985) The role of fractional crystallization in the evolution of the Nandewar Volcano, North-eastern New South Wales, Australia. J Petrol 26:1002–1026

Stolz AJ (1986) Mineralogy of the Nandewar Volcano, northeastern New South Wales, Australia. Mineral Mag 50:241–255

Sun SS (1980) Lead isotopic study of young volcanic rocks from mid-ocean ridges, ocean islands and island arcs. Phil Trans R Soc Lond A 297:409–445

Takahashi E, Kushiro I (1983) Melting of a dry peridotite at high pressures and basalt magma genesis. Am Mineral 68:859–879

Thompson RN (1982) Magmatism of the British Tertiary Volcanic Province. Scott J Geol 18:49–107

Varne R, Foden JD (1986) Geochemical and isotopic systematics of eastern Sunda arc volcanics: implications for mantle sources and mantle mixing processes. In: Wezel FC (ed) The Origin of Arcs. Elsevier, Amsterdam, pp 159–189

Venturelli G, Capedri S, Di Battistini G, Crawford AJ, Kogarko LN, Celestini S (1984) The ultrapotassic rocks from southeastern Spain. Lithos 17:37–54

Ware NG (1981) Computer programs and calibration with the PIBS technique for quantitative electron probe analysis using a lithium-drifted silicon detector. Computers and Geosciences 7:167–184

Whitford DJ (1975a) Geochemistry and petrology of volcanic

rocks from the Sunda arc, Indonesia. Unpublished Ph.D. thesis, Australian National University, p 449
Whitford DJ (1975b) Strontium isotopic studies of the volcanic rocks of the Sunda arc, Indonesia, and their petrogenetic implications. Geochim Cosmochim Acta 39:1287–1302
Whitford DJ, Foden JD, Varne R (1978) Sr isotope geochemistry of calcalkaline and alkaline lavas from the Sunda arc in Lombok and Sumbawa, Indonesia. Carneg Inst Wash Ybk 77:613–620
Whitford DJ, Nicholls IA, Taylor SR (1979) Spatial variations in the geochemistry of Quaternary lavas across the Sunda arc in Java and Bali. Contrib Mineral Petrol 70:341–356
Whitford DJ, White WM, Jezek PA (1981) Neodymium isotopic composition of Quaternary island arc lavas from Indonesia. Geochim Cosmochim Acta 45:989–995
Wilkinson JFG, Stolz AJ (1983) Low-pressure fractionation of strongly undersaturated alkaline ultrabasic magma: the olivine-melilite-nephelinite at Moiliili, Oahu, Hawaii. Contrib Mineral Petrol 83:363–374
Zindler A, Hart SR (1986) Chemical geodynamics. Ann Rev Earth Planet Sci 14:493–571

Received June 10, 1987 / Accepted December 7, 1987

Editorial responsibility: T. Grove